Supplementary Information

Development of a tannic acid and silicate ions functionalized PVA-starch composite hydrogel for in situ skeletal muscle repairing

Longkang Li,[‡a] huipeng Li,[‡b] Zhentian Diao,[a] Huan Zhou,[*b] Yanjie Bai[*c] and Lei Yang[b]

[a]School of Materials Science and Engineering, Hebei University of Technology, Tianjin, 300130, China.

[b]Center for Health Science and Engineering, Hebei Key Laboratory of Biomaterials and Smart Theranostics, School of Health Sciences and Biomedical Engineering, Hebei University of Technology, Tianjin, 300130, China. E-mail: zhouhuan@hebut.edu.cn (Huan Zhou).

[c]Department of Chemical Engineering, Hebei University of Technology, Tianjin, 300130, China. E-mail: 2021100@hebut.edu.cn (Yanjie Bai).

[‡]These authors contributed equally to this work.

*Co-corresponding authors.

1.Adhesion testing

The adhesion of different types of PSTS to different substrates was quantitatively tested using a mechanical tester by fixing the substrate material in the upper and lower fixtures of the mechanical tester. The PSTS was placed on the surface of the substrate in the lower fixture. The upper fixture was moved downwards until it came into contact with the PSTS and generated 2 N of pressure. When the pressure was relaxed to 0 N, the upper and lower substrate materials were separated by stretching at a rate of 20 mm/min, and the maximum stress during the separation was defined as the adhesion strength.

2.PSTS intracellular ROS generation assay

C2C12 myoblasts were inoculated in 24-well plates (2.5×10^4 cells/well), after the cells were attached to the wall, hydrogel extract or fresh DMEM was used instead of medium, and 250 mM H_2O_2 was added to induce oxidative stress, and the incubation was continued for 24 h. The medium was removed, and dichlorofluorescein dichloride 20,70 bis(acetate)-diacetate (DCFH) diluted in serum-free medium (1:1000) and incubated at 37 ℃ for 30 min. cells were imaged using an inverted fluorescence microscope.

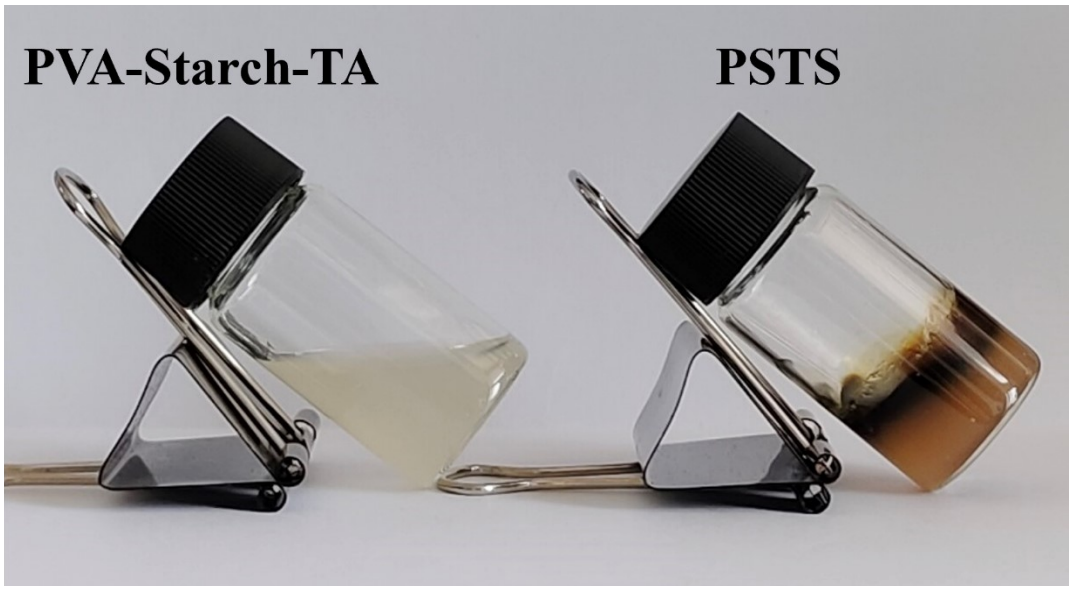

Figure S1. Comparison of hydrogel forming properties of PVA-Starch-TA and PSTS.

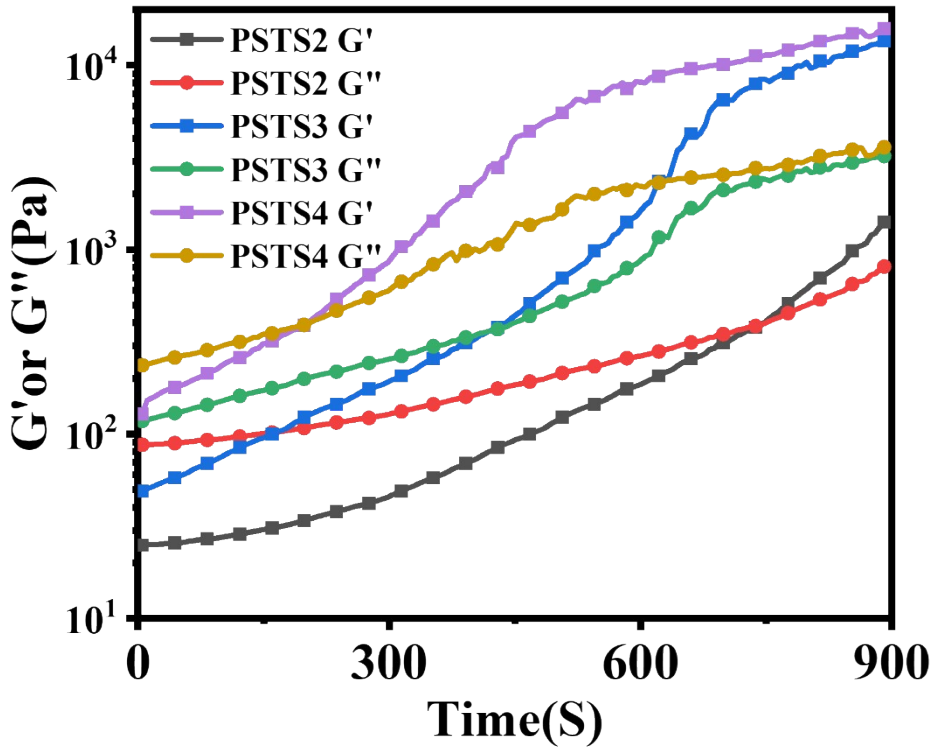

Figure S2. Rheogram of gelation time for different concentrations of PSTS.

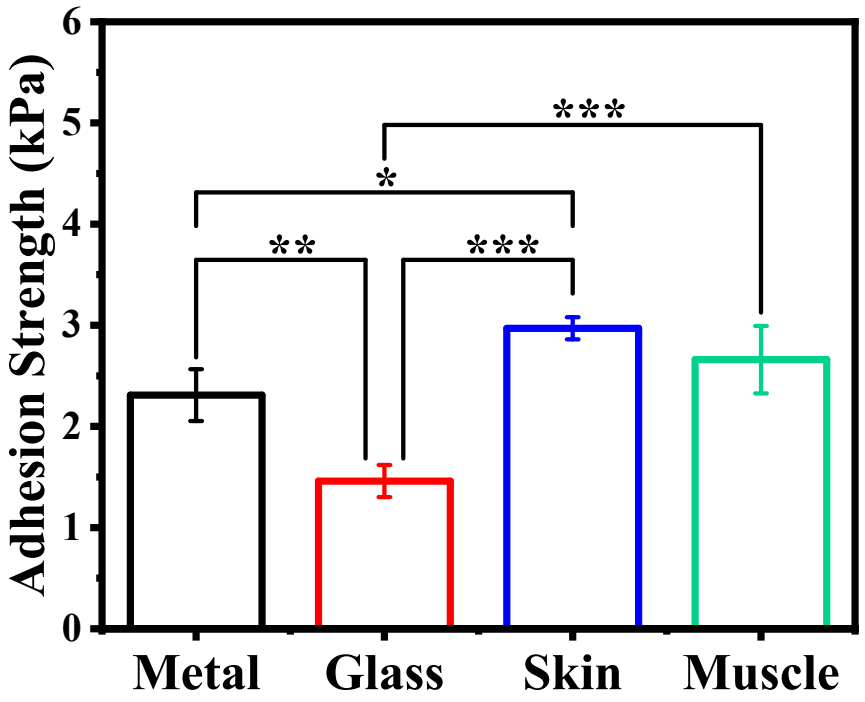

Figure S3. Adhesion ability of PSTS on different substrate surfaces. *(*p < 0.05; ***p < 0.001)*.

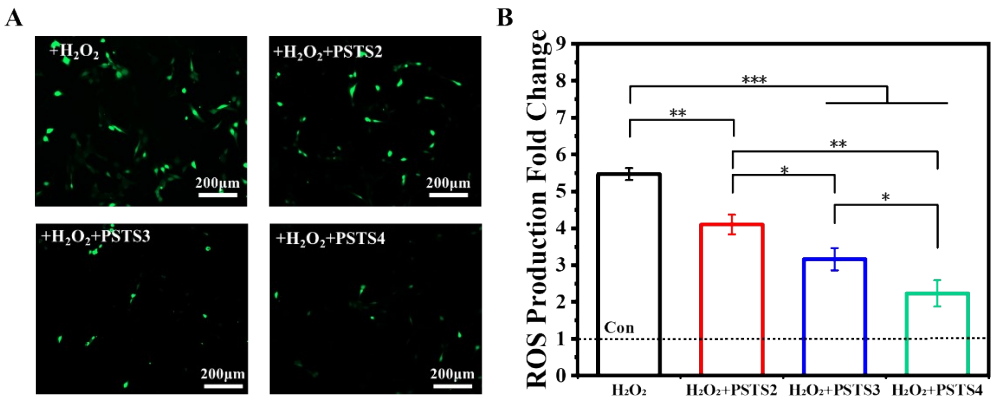

Figure S4. PSTS inhibits intracellular ROS generation (A) DCFH probe detects ROS levels (ROS: green) in C2C12 myoblasts after addition of H2O2 and incubation in conventional medium or hydrogel extracts for 1 day, (B) Quantification of intracellular ROS intensity. *(*p < 0.05; **p < 0.01; ***p < 0.001)*.

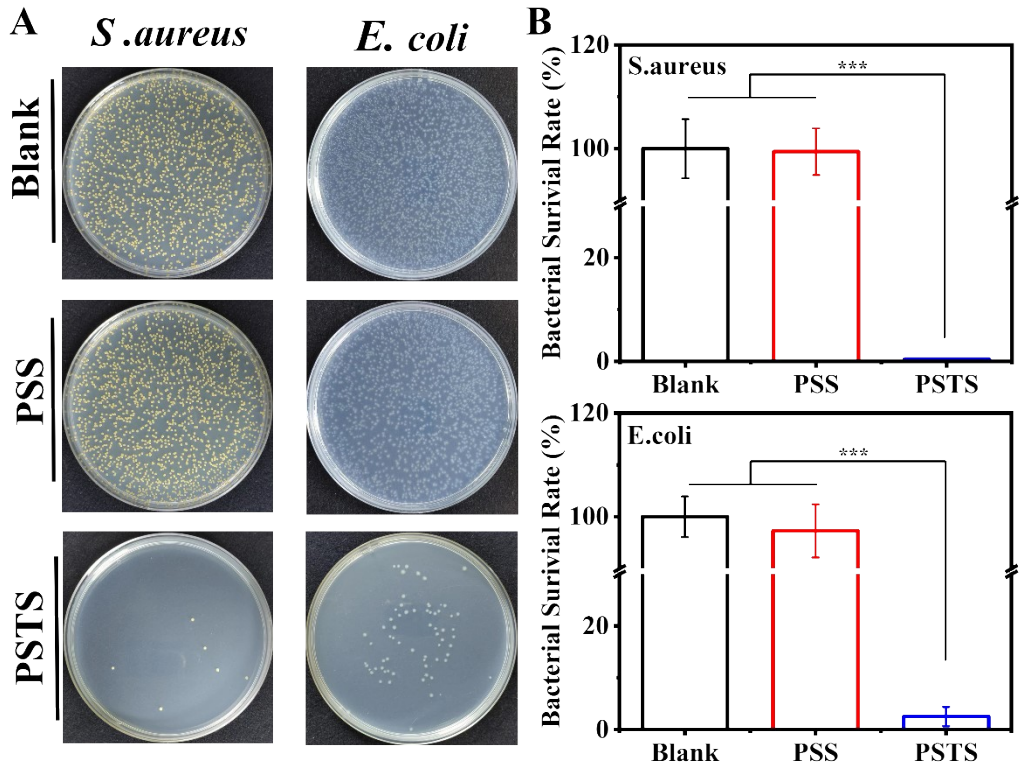

Figure S5. Comparison of antimicrobial properties of TA-free hydrogel (PSS) and PSTS. *(***$p < 0.001$).*

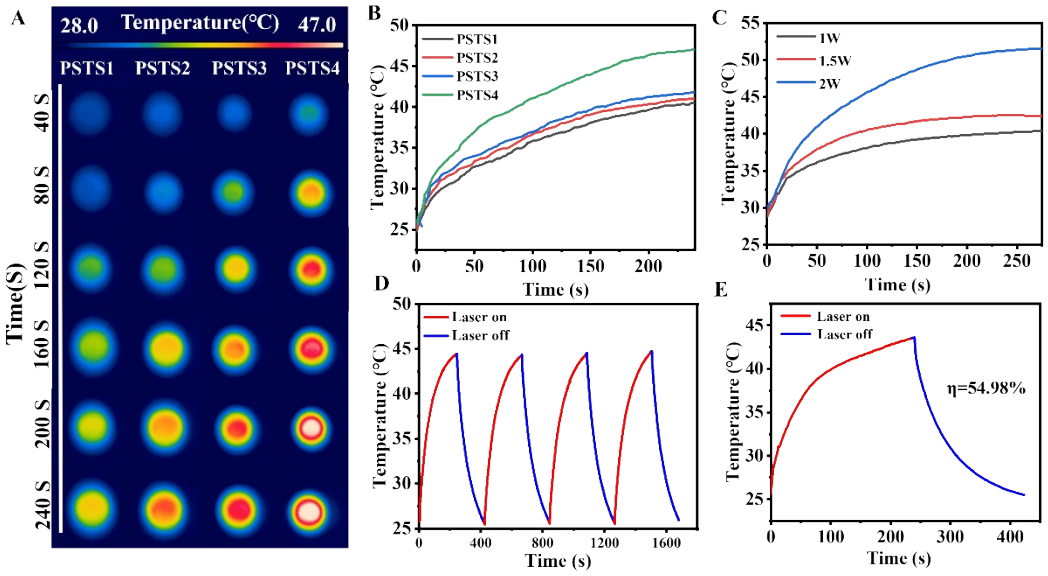

Figure S6. Photothermal performances of PSTS hydrogels. (A) Photothermal images with infrared camera. (B) Temperature and time variation of PSTS hydrogels under NIR. (C) Temperature and time variation of PSTS2 hydrogel under NIR with different power. (D) Cyclic photothermal behavior of PSTS2 hydrogel (Laser on 4min, Laser off 3min). (E) A photothermal cycle of PSTS2 hydrogel at 1.5W NIR (Laser on 4min, Laser off 3min).

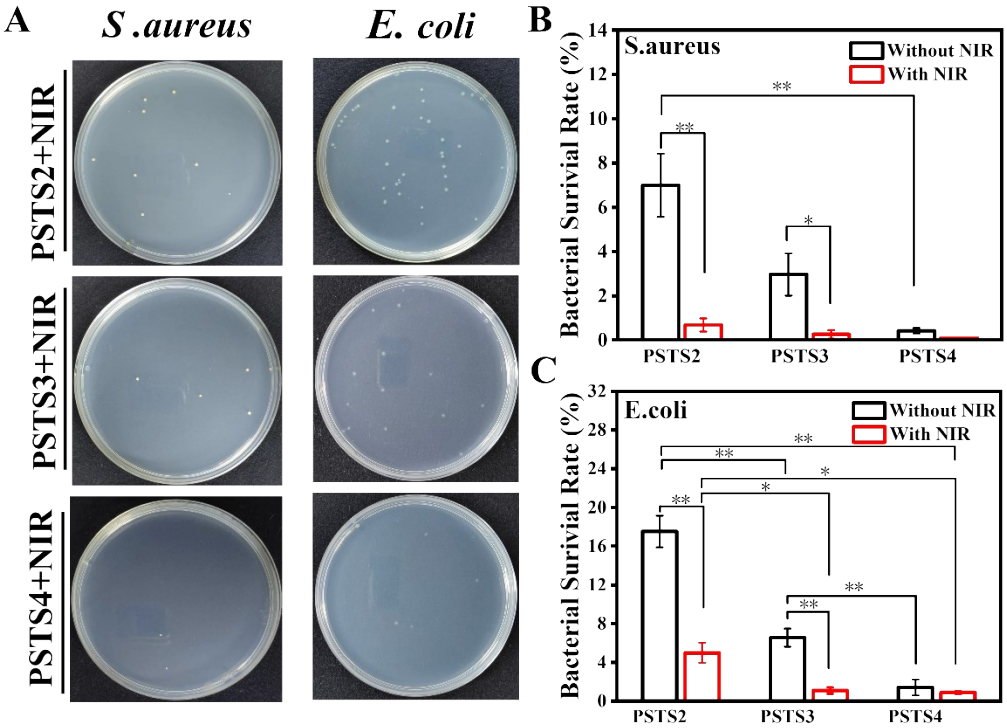

Figure S7. Bacterial inhibitory activity evaluation of PSTS hydrogel after NIR. (A) Photographs of colonies of *Staphylococcus aureus* and *Escherichia coli* after contact with different PSTS hydrogels after NIR. (B) Survival rate of *Staphylococcus aureus* was significantly reduced when PSTS was empowered with NIR irradiation. (C) Survival rate of *E. coli* was significantly reduced when PSTS was empowered with NIR irradiation *(*p < 0.05; **p < 0.01; ***p < 0.001).*

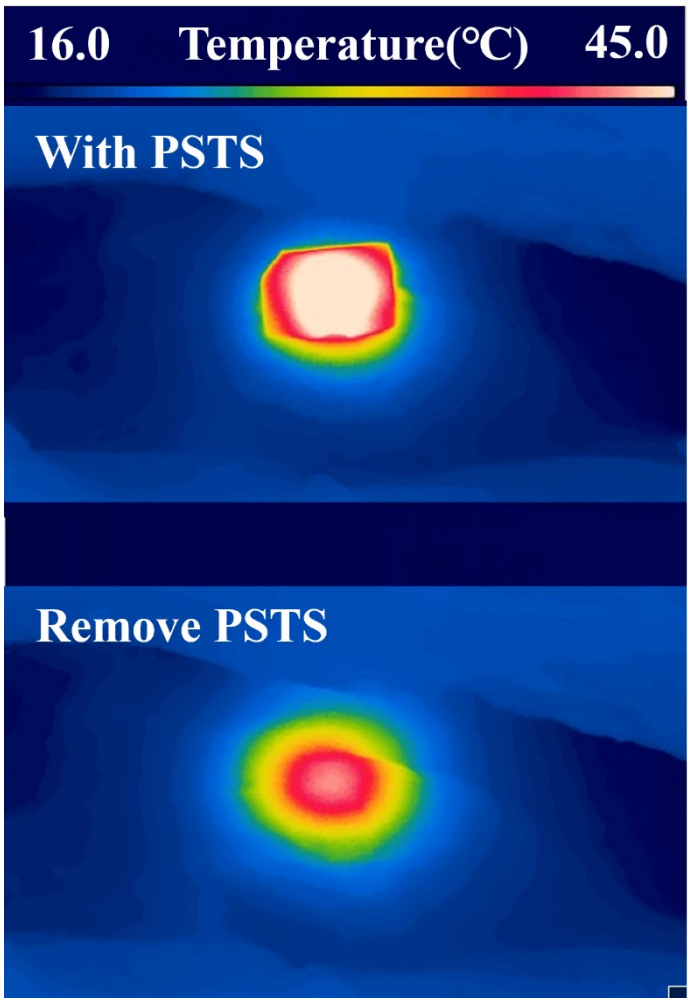

Figure S8. PSTS covering the muscle surface influences muscle warming through NIR.